

PREPARATION & CHARACTERIZATION OF Co/Zn CATALYST, SBA-15  
SUPPORTED FOR FISHER TROPSCH SYNTHESIS: EFFECT OF COBALT  
LOADING

MOHAMMAD FAIRUZ BIN MOHAMMAD NAFFEKYUDIN

UNIVERSITI MALAYSIA PAHANG

# UNIVERSITI MALAYSIA PAHANG

## BORANG PENGESAHAN STATUS TESIS♦

JUDUL: PREPARATION & CHARACTERIZATION OF Co/Zn CATALYST,SBA-15 SUPPORTED FOR FISHER TROPSCH SYNTHESIS:EFFECT OF COBALT LOADING

SESI PENGAJIAN : 2010/2011

Saya MOHAMMAD FAIRUZ BIN MOHAMMAD NAFFEKYUDIN

(HURUF BESAR)

mengaku membenarkan tesis (PSM/~~Sarjana/Doktor Falsafah~~)\* ini disimpan di Perpustakaan Universiti Malaysia Pahang dengan syarat-syarat kegunaan seperti berikut :

1. Tesis adalah hakmilik Universiti Malaysia Pahang
2. Perpustakaan Universiti Malaysia Pahang dibenarkan membuat salinan untuk tujuan pengajian sahaja.
3. Perpustakaan dibenarkan membuat salinan tesis ini sebagai bahan pertukaran antara institusi pengajian tinggi.

4. \*\*Sila tandakan ( √ )

SULIT

(Mengandungi maklumat yang berdarjah keselamatan atau kepentingan Malaysia seperti yang termaktub di dalam AKTA RAHSIA RASMI 1972)

TERHAD

(Mengandungi maklumat TERHAD yang telah ditentukan oleh organisasi/badan di mana penyelidikan dijalankan)

TIDAK TERHAD

Disahkan oleh

\_\_\_\_\_  
(TANDATANGAN PENULIS)

\_\_\_\_\_  
(TANDATANGAN PENYELIA)

Alamat Tetap: Kampung Bukit Lada,

Nurul Sa'aadah Sulaiman

Jln Kubur Panjang

(Nama Penyelia)

06400 Pokok Sena, Kedah.

Tarikh : 2 DECEMBER 2010

Tarikh: 2 DECEMBER 2010

CATATAN :

\*

Potong yang tidak berkenaan.

\*\*

Jika tesis ini **SULIT** atau **TERHAD**, sila lampirkan surat daripada pihak berkuasa/organisasi berkenaan dengan menyatakan sekali sebab dan tempoh tesis ini perlu dikelaskan sebagai **SULIT** atau **TERHAD**.

♦

Tesis dimaksudkan sebagai tesis bagi Ijazah Doktor Falsafah dan Sarjana secara penyelidikan, atau disertasi bagi pengajian secara kerja kursus dan penyelidikan, atau Laporan Projek Sarjana Muda (PSM).

“I/we hereby declare that I/we have read this thesis and in my/our opinion this thesis has fulfilled the qualities and requirements for the award of Degree of Bachelor of Chemical Engineering (~~Chemical/Bio~~technology/GasTechnology)”

Signature : .....

Name of Supervisor : NURUL SA’AADAH BINTI SULAIMAN

Date : .....

**PREPARATION AND CHARACTERIZATION OF SBA-15 SUPPORTED Co/Zn  
CATALYST FOR FISHER TROPSCH SYNTHESIS: EFFECT OF COBALT  
LOADING**

**MOHAMMAD FAIRUZ BIN MOHAMMAD NAFFEKYUDIN**

**A thesis submitted in fulfillment  
of the requirements for the award of the Degree of  
Bachelor of Chemical Engineering (Gas Technology)**

**Faculty of Chemical & Natural Resources Engineering  
Universiti Malaysia Pahang**

**DECEMBER 2010**

“I declare that this thesis entitled “Preparation and Characterization of SBA-15 Supported Co/Zn Catalyst for Fisher Tropsch Synthesis: Effect of Cobalt Loading” is the result of my own research except as cited in references. The thesis has not been accepted for any degree and is not concurrently submitted in candidature of any other degree.”

Signature : .....

Name : MOHAMMAD FAIRUZ BIN MOHAMMAD NAFFEKYUDIN

Date : 2 DECEMBER 2010

*To my family*

Thank you for the support, encouragement and motivation that have been given

*To all my friends*

Thank you for the support and assistance that have been given

## ACKNOWLEDGEMENT

In the early stage of my research and in organizing my thoughts on the thesis, I have benefited greatly from discussions with a number of researchers, academicians and practitioners. In particular, I wish to express my sincere appreciation to my main thesis supervisor, Madam Nurul Sa'adah Binti Sulaiman for encouragement, guidance, critics and support from the initial to the final level enabled me to develop an understanding of the subject.

Besides that, I would like to express my thanks to my loving mother and father respectively, Madam Izah Ahmad and Mr. Mohammad Naffekyudin Bin Yaacob who are very supportive morally.

My fellow friends especially Mohammad Zakwan Bin A Razak and Nor Hayati Binti Zulkifli should also be recognized for their support. Their views and support are useful indeed.

I would like to thanks Madam Hafiza Binti Ramli and Mr. Masri Bin Abdul Razak as the Teaching Engineer in Analytical Lab and Gas Lab for their guidance and technical support. Without their continued support and interest, this thesis would not have been the same as presented here. Unfortunately, it is not possible to list all of them in this limited space. Not to forget the lecturers from Faculty of Chemical and Natural Resources Engineering who had teach me all this while.

Lastly, I offer my regards and blessings to all of those who supported me in any respect during the completion of the project.

## ABSTRACT

The influence of promoter (Zn) and effect of cobalt loading on the physiochemical and catalytic properties of mesoporous silica Co/SBA-15 catalysts for the Fischer-Tropsch (FT) synthesis was investigated. SBA-15 was synthesized as support. The mesoporous silica Co-Zn/SBA-15 catalysts were prepared by incipient wetness impregnation method. Cobalt nitrate and zinc nitrate were used as sources of metal that introduced onto support with same zinc loading (20 wt %) and different cobalt loading (5 wt %, 10 wt%, 15 wt %). The characterization of catalysts was performed by using Fourier transform Infrared (FTIR) and Scanning Electron Microscopy (SEM). The results for FTIR were identification of Si-O-Zn and Si-O-Co functional group because of the present of zinc or cobalt onto silica SBA-15 support. Besides that, the identification of metal inside SBA-15 was determined by comparing the pure SBA-15 with the incorporated metal on SBA-15. For SEM analysis, the image shows that the rope like domain aggregated to wheat like microstructure. Incorporation of Co and Zn did not change the morphology of the support. For this research, the characterization of the catalyst by selecting Zn as promoter have quiet similar characterization with noble metal that already investigate.



## ABSTRAK

Pengaruh zink sebagai penyumbang dan pengaruh kehadiran kobalt pada sifat-sifat fizikal dan kimia dan sifat katalitik dari mangkin silika Co/SBA-15 berliang meso untuk Fischer-Tropsch (FT) sintesis telah diteliti. SBA-15 disintesis sebagai penyokong/pendukung. Pemangkin silika berliang meso Co-Zn/SBA-15 disediakan dengan kaedah impregnasi yang sedikit basah. Cobalt nitrat dan zink nitrat digunakan sebagai sumber logam untuk menghasilkan pemangkin. Kuantiti zink yang dimasukkan adalah sama (20 wt% ) dan kuantiti kobalt yang berbeza (5 wt%, 10% wt, 15% wt). Sifat-sifat mangkin di percirikan dengan menggunakan transformasi Fourier Infrared (FTIR) dan Mikroskop Elektron (SEM). Keputusan untuk FTIR adalah pengenalan Si-O-Zn dan Si-O-Co kumpulan berfungsi kerana zink atau kobalt hadir di atas SBA-15. Selain itu, pengenalan logam di dalam SBA-15 juga ditentukan dengan membandingkan SBA-15 dengan SBA-15 yang diimpregnasikan dengan unsur logam. Untuk analisis SEM, gambarajah menunjukkan sifat SBA-15 dan SBA-15 yang telah diimpregnasikan dengan logam bersifat seperti lingkaran tali yang berpintal dan pengaruh Zn dan Co tidak sama sekali mengubah bentuk morfologi penyokong . Untuk kajian ini, didapati ciri-ciri mangkin dengan pemilihan Zn sebagai unsur penggalak mempunyai ciri-ciri yang sama dengan logam aktif yang telah digunakan sebelum ini .

## TABLE OF CONTENTS

CHAPTER	TITLE	PAGE
	<b>DECLARATION</b>	<b>ii</b>
	<b>DEDICATION</b>	<b>iii</b>
	<b>ACKNOWLEDGEMENTS</b>	<b>iv</b>
	<b>ABSTRACT</b>	<b>v</b>
	<b>ABSTRAK</b>	<b>vi</b>
	<b>TABLE OF CONTENTS</b>	<b>vii</b>
	<b>LIST OF TABLES</b>	<b>ix</b>
	<b>LIST OF FIGURES</b>	<b>x</b>
	<b>LIST OF ABBREVIATION</b>	<b>xi</b>
	<b>LIST OF APPENDICES</b>	<b>xii</b>
<b>1.</b>	<b>INTRODUCTION</b>	
	1.1 Background of study	1
	1.1.1 Fisher-Tropsch Process	1
	1.1.2 Catalyst for Fisher-Tropsch	3
	1.1.3 Application of Fisher-Tropsch	4
	1.2 Problem statement	6
	1.3 Objectives of the study	7
	1.4 Scope of study	7
<b>2.</b>	<b>LITERATURE REVIEW</b>	
	2.1 Cobalt Based Catalyst	9
	2.2 SBA-15	10
	2.3 Effect of Cobalt Loading	14

2.4	Effect of Zinc Promoter	15
	2.4.1 Cobalt Dispersion	16
	2.4.2 Cobalt Reducibility	17
	2.4.3 Enhancement of Catalytic Performance	18
2.5	Ways for Functionalization of Catalyst	19
2.6	Catalyst Characterizations	22
	2.6.1 Thermogravimetric Analysis (TGA)	22
	2.6.2 N <sub>2</sub> Adsorption Analysis	24
	2.6.3 Fourier Transform Infrared (FTIR)	25
	2.6.4 Scanning Electron Microscopy (SEM)	27
<b>3.</b>	<b>MATERIALS AND METHODOLOGY</b>	
	3.1 Introduction	28
	3.2 Materials and Chemicals	29
	3.3 SBA-15 preparation	29
	3.4 Co-Zn /SBA-15 Synthesis	30
	3.5 Catalyst characterization	30
<b>4.</b>	<b>RESULT AND DISCUSSION</b>	
	4.1 Scanning Electron Microscopy (SEM)	32
	4.2 Fourier Transform Infrared (FTIR)	34
<b>5.</b>	<b>CONCLUSION AND RECOMMENDATIONS</b>	
	5.1 Conclusion	39
	5.2 Recommendations	40
	<b>REFERENCES</b>	41
	<b>APPENDICES A</b>	48

**LIST OF TABLES**

<b>TABLE NO.</b>	<b>TITLE</b>	<b>PAGE</b>
<b>1.1</b>	Comparison of Cobalt and Iron FT Catalysts (Khodakov <i>et al.</i> , 2007)	4
<b>1.2</b>	Uses and applications products from FT reaction (Shalchi, 2006)	6
<b>2.1.</b>	Chemical composition and textural properties SBA-15-supported Co catalysts (Martinez <i>et al.</i> , 2003)	24
<b>3.1</b>	List of Chemicals	29
<b>3.2</b>	Percentage of metal loading in the SBA-15	30

**LIST OF FIGURES**

<b>FIGURE NO.</b>	<b>TITLE</b>	<b>PAGE</b>
1.1	Developers of the Fischer -Tropsch Synthesis Process	1
1.2	Percentages of the GTL products ( Shalchi, 2006).	5
2.1	Synthesis of SBA-15 mesoporous silica (Mukaddes, 2005)	11
2.2	TEM images of pure SBA-15(Akca, 2006)	12
2.3	Schematic ways of functionalization mesoporous material (Taguchi <i>et al.</i> , 2005)	21
2.4	DSC-TGA curves of cobalt silica-supported catalyst (Girardon <i>et al.</i> , 2007)	23
2.5	FTIR spectra in the C–H stretching region of SBA-15 with OTS adsorption showing –CH <sub>2</sub> and –CH <sub>3</sub> stretching bands	26
2.6	SEM microphotographs (Anunziata <i>et al.</i> , 2007)	27
3.1	Flow chart overall experimental work.	28
4.1	SEM monograph of mesoporous SBA-15	32
4.2	FT-IR spectra	35

**LIST OF ABBREVIATIONS**

<b>FTIR</b>	Fourier Transform infrared Spectra
<b>TGA</b>	Thermogravimetric Analysis
<b>SEM</b>	Scanning Electron Microscopy
<b>FT</b>	Fisher Tropsch
<b>WGS</b>	Water Gas Shift
<b>TEM</b>	Transmission Electron Microscopy
<b>SCR</b>	Selective Catalytic Reduction
<b>Zn</b>	Zinc
<b>Co</b>	Cobalt
<b>Al<sub>2</sub>O<sub>3</sub></b>	Alumina
<b>CoO</b>	Cobalt Oxide
<b>TEOS</b>	Tetraethylorthosilicate
<b>MSI</b>	Metal Surface Interaction
<b>XRD</b>	X-Ray Diffraction
<b>GTL</b>	Gas to liquid

**LIST OF APPENDIX**

<b>FIGURE</b>	<b>TITLE</b>	<b>PAGES</b>
A1	Calculation of wt % zinc and cobalt loading using during incipient wetness impregnation method.	48

## CHAPTER 1

### INTRODUCTION

#### 1.1 Background of the study

##### 1.1.1 Fisher-Tropsch Process

In 1902, Paul Sabatier and Jean Sanderens discovered a way of converting Carbon Monoxide (CO) and Hydrogen (H<sub>2</sub>) to Methanol (CH<sub>3</sub>OH) (Hill,1982). Franz Fischer and Hans Tropsch developed this synthesis to mainly oxygenated products and hydrocarbons in 1923 using alkalized iron as a catalyst (Davis, 1997). In 1925 the two German scientists further developed this reaction by converting the mixture of (CO) and (H<sub>2</sub>) which is called Synthesis Gas or "Syngas" in a laboratory to oxygenated products and liquid hydrocarbons using cobalt and nickel catalysts at atmospheric pressures.



**Figure 1.1:** Developers of the Fischer -Tropsch Synthesis Process (Shalchi, 2006)



In order to commercialize the FT reaction to become FT process, the production of raw hydrocarbons can be refined and upgraded into different fuels like gasoline, diesel, and other products. In the mid 1930s, a number of Fischer-Tropsch plants were constructed, and by 1938, over 590,000 tons of oil and gasoline were being produced annually in Germany from synthesis gas manufactured from coal.

During 1930s, plants were also constructed in Japan, Britain, and France. During World War II Germany operated nine F-T plants that produced 12,000 barrel/day of fuel. Those plants that were not destroyed during the war were shut down subsequently as cheap petroleum crude and natural gas became available. One country which has continued to pursue the development of indirect coal liquefaction by Fischer-Tropsch process is South Africa.

In the following years many companies like Mobile, Sasol, Shell, Rentech, ConocoPhillips, Syntroleum, and BP, have started technology developments of the Fischer-Tropsch process either in response to oil crises, or due to high crude oil price. The main purpose of these developments is to make any industrial plant use this technology to become commercially successful.

Fischer-Tropsch Synthesis (F-T) converts synthesis gas ( $\text{CO}$  and  $\text{H}_2$ ) which can be made from coal, natural gas, petroleum residues, biomass, and any carbonaceous materials to long chain hydrocarbons. If liquid petroleum-like fuel, lubricant, or wax is required, then the Fischer-Tropsch process is the right process that can be applied. This is an alternative route to obtain fuels and chemicals rather than the current dominant petroleum resources. Fischer-Tropsch synthesis now is becoming competitive to petroleum due to its improved catalysts and processes (Shalchi, 2006).

Currently, Gas to Liquids (GTL) is the major focus on the (F-T). Chemically the (GTL) in Fischer-Tropsch process is a series of catalyzed chemical reactions in which carbon monoxide and hydrogen are converted into liquid hydrocarbons of various

forms. The principal purpose of this process as mentioned above is to produce a synthetic petroleum substitute. The original basic Fischer-Tropsch process is as follows by equation (1) and (2):



FT synthesis have been realized recently (Bintulu in Malaysia, Oryx in Qatar) or are currently under construction (Pearl in Qatar, Escravos in Nigeria). The world consumption of crude oil in 2015 can be estimated as 20 million barrels per day. (Liang *et al.*, 2007).

FT synthesis was used in Germany during World War II to produce fuels from coal, and has been employed in SASOL, South Africa since the 1950s to produce fuels and chemicals. Shell has built a plant in Malaysia as a showcase of modern FT technology based on natural gas. Recently California air and energy officials in a California Air Resources Board (CARB) symposium praised the potential for gas-to-liquids (GTL), essentially FT synthesis, to make a significant future contribution to the state's diesel supply while reducing emissions and dependence on petroleum-based (shalchi, 2006).

### 1.1.2 Catalyst for Fisher-Tropsch

Cobalt and iron are the metals that were proposed by Fischer and Tropsch as the first catalysts for syngas conversion. Both cobalt and iron catalysts have been used in the industry for hydrocarbon synthesis. A brief comparison of cobalt and iron catalysts is given in Table 1.1.

**Table 1.1:** Comparison of Cobalt and Iron FT Catalysts (Khodakov *et al.*, 2007)

Parameter	Cobalt catalysts	Iron catalyst
Cost	More expensive	Less expensive
Lifetime	Resistance to deactivation	Less resistance to deactivation
Activity at low conversion	Comparable	Comparable
Productivity at high conversion	Higher, less significant effect of water on the rate of carbon monoxide conversion	Lower, strong negative effect of water on the rate of carbon
Maximal chain growth probability	0.94	0.95
water gas shift reaction $\text{CO} + \text{H}_2\text{O} \rightarrow \text{CO}_2 + \text{H}_2$	Not very significant, more noticeable at high conversion	Significant
Maximal sulphur content	<0.1 ppm	<0.2 ppm
Flexibility (temperature and pressure)	Less flexible, significant influence of temperature and pressure on hydrocarbon selectivity	Flexible, methane selectivity is relatively low even at 613K

### 1.1.3 Application of Fisher-Tropsch Process and Product

In the twenty first-century, natural gas is expected to become an increasingly important raw material for manufacturing clean fuel and chemical. Fisher-Tropsch synthesis is the major part of gas to liquid technology, which is convert natural gas

into liquid fuel with very low sulphur and aromatic compound. Generally, the liquid fuels producing from GTL Technology consist of Synthetic LPG, Synthetic Naphtha, Synthetic Kerosine and Synthetic Diesel. Figure 1.2 shows the percentage of GTL products.

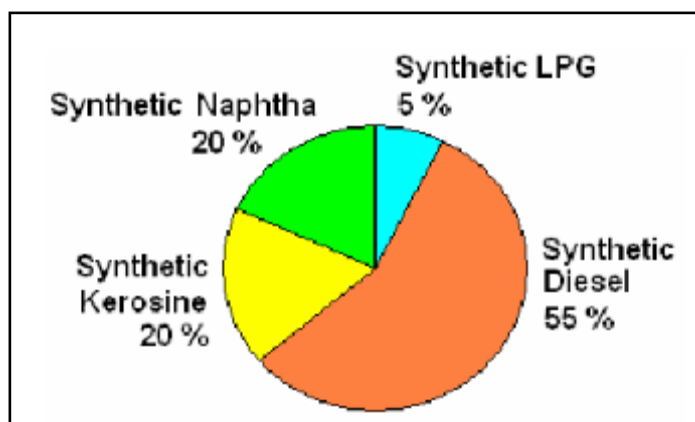


**Figure 1.2:** Percentages of the GTL products ( Shalchi, 2006).

There is much factor that gives impact to the percentage of these product increases or decreases. The percentage of these products increase or decrease according to the kind of technology employed, nature of the catalyst, and the conditions of the reactions used. The properties of the GTL products are typical with regard of its combustion or its environmental affects. Since the light and mid synthetic products are the main and the most important products of the GTL industry. Therefore the significant care of the properties of these products play a great role in the promotion of the GTL industry (Shalchi, 2006).

The benefits of Fischer-Tropsch reactions is not restricted to producing valuable light and mid petroleum derivatives, but it also used to produce many valuable chemicals by only altering the operation conditions to change the growth of the hydrocarbon chains. Typical uses and applications are mentions on table 1.2 for other derivatives produced from fisher tropsch process that are valuable for daily life.

**Table 1.2:** Shows the typical uses and applications for different products produce after Fisher-Tropsch reaction (Shalchi, 2006):

<b>Product Group</b>	<b>Typical uses and applications</b>
Normal Paraffin's	Production of intermediates (LAB, SAS, alcohols). Production of intermediates for plasticizers, auxiliary chemical, manufacturing of film and special catalyst carrier and low polar odor-free all purposes solvents and diluents.
Mixed Paraffin's	Special low polar and odor-free solvent for paints, coating, dry cleaning, cleaners, insecticide and pesticide formulation, and drilling fluids.
Synthetic lubricants	Industrial and automotive lubricant applications including motor oils, compressor oil, hydraulic fluids, and grease.
Paraffin Wax	Manufacturing of candies, crayons, printing inks, potting and cables compounds, coatings, and packaging

## 1.2 Problem Statement

Catalyst is a vital part of any industrial FT process. FT process is a method for production of hydrocarbons from synthesis gas. The supported cobalt catalysts have been extensively used in FT process and have been found to be particularly convenient for the production of high hydrocarbons. In the future of industry, iron, cobalt and ruthenium are the best catalysts for FT synthesis polymers (Mukaddes, 2005).

But among them, cobalt catalysts are the preferred catalysts for FT synthesis based on natural gas because of their high activity for FT synthesis, high selectivity to linear hydrocarbons, low activity for the water gas shift (WGS) reaction, more stability toward deactivation by water (a by-product of the FT reaction), and low cost compared to Ru (Tavasoli *et al.*, 2007).

The use of periodic mesoporous silica as supports for preparing Co-based FT synthesis catalysts has been recently explored by many researches because mesoporous have very high surface area characteristic that will allow high dispersions at higher cobalt loading as compared with conventional amorphous silicas (Martinez *et al.*, 2003). In this research SBA-15 was used as a mesoporous silica support.

Numerous studies show that introduction of noble metals (Ru, Rh, and Pt) has strong impact on the structure and dispersion of cobalt species and FT reaction rates (Khodakov, 2009). But recently this noble's metal are higher in cost (Zhang *et al.*, 2003). As example Shell's plant in Malaysia employs cobalt catalysts. Ruthenium catalysts have excellent FT reactivity; however, no commercial ruthenium catalyst has ever been used, mainly due to its high cost. Ruthenium, zinc and has been used to improve the reduction and reactivity of cobalt catalysts (Zhang *et al.*, 2003). Thus, zinc was used as noble metal in this research because it's low price than other.

### **1.3 Objective**

The objectives of this research are:

- i. To synthesis SBA-15 as a support for catalyst.
- ii. To synthesis Co-Zn/SBA-15 catalyst and study the effect of Co loading.
- iii. To characterized Co-Zn/SBA-15 catalysts.

### **1.4 Scope of Study**

To achieve the objectives, scopes have been identified in this research. Generally, the scopes of this research are focus on producing the new catalyst for FT synthesis which is Co-Zn/SBA-15 and the influence of cobalt and zinc promoter load

was investigated. Co-Zn/SBA-15 catalysts with same Zn defined with porous surface contents which 20 wt% and different Co contents which range 5 wt % until 15 wt % were prepared by incipient wetness impregnation of relative SBA-15 with desired amount of aqueous cobalt nitrate and zinc nitrate. The samples Co-Zn/SBA-15 catalyst was then characterized using Fourier Transform Infrared analysis (FTIR) and Scanning Electron Microscopy (SEM).

## CHAPTER 2

### LITERATURE REVIEW

#### 2.1 Cobalt based catalyst

The FT synthesis process was shown to be catalyzed by certain transition metals, with Co, Fe, and Ru presenting the highest activity (Vannice, 1977). Among them, cobalt-based FT synthesis catalysts are usually preferred for the synthesis of long-chain paraffins (Iglesia *et al.*, 1997) as they are more active per weight of metal, more efficient deactivation by water (a by-product of the FT synthesis reaction), less active for the competing water-gas shift (WGS) reaction, and produce less oxygenates than the iron-based systems. Ru-based catalysts are highly active but the high cost and low availability of Ru are important concerns limiting their commercial application (Schultz, 1999).

Significant efforts have focused on the optimization and tailoring of cobalt catalysts for specific applications. It has been demonstrated that cobalt active component, support, and promoter have important effects on the catalyst performance and structure (Schultz, 1999). Iglesia *et al.* (1997) reported that for relatively large cobalt particles (diameter > 10 nm), FT reaction rates were proportional to metal dispersion. Bartholomew (1984), Yermakov (1984), and De Jong (2006) observed that lower FT turnover frequencies with cobalt particles smaller than 6–8 nm. It seems that lower activity of small cobalt particles might be attributed to both their reoxidation at



the reaction conditions and modified electronic structure because of the quantum size effect.

A recent report by Loosdrecht (2007) reinforces that currently there is no consistent picture regarding oxidation of cobalt particles during FT reaction it was shown that reoxidation of cobalt metal particles in industrial FT reactors could be prevented by efficient control of water and hydrogen pressures. Thus, the observed decrease in FT productivity during the reaction likely cannot be assigned solely to cobalt particle oxidation. Analysis of the literature suggests that a highly active cobalt catalyst would require optimal-sized of cobalt metal particles, high reducibility, and high stability of cobalt active sites.

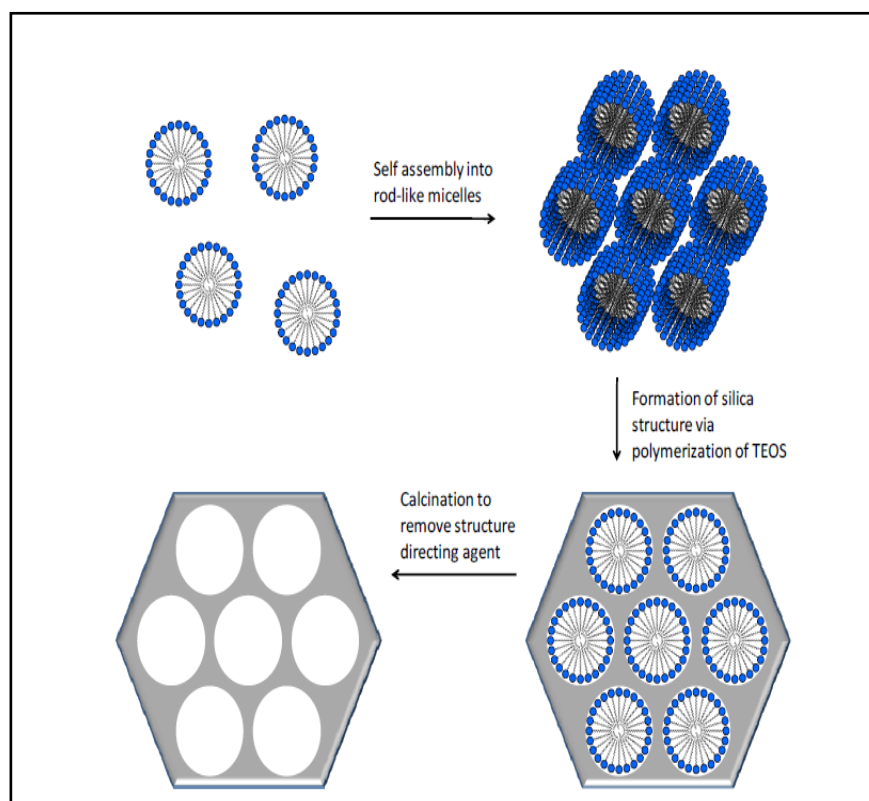
## **2.2 SBA-15 Supported cobalt based catalyst**

SBA-15 is one member of a family of mesoporous silicas that make ideal candidates for catalyst supports by covalent grafting (Wight *et al.*, 2002). It is an ordered, amorphous silica material first created by Zhao and Stucky in 1998, in an effort to increase the material's thermal stability via increased wall thickness relative to MCM type materials. The improved hydrothermal and thermal stability makes them the most promising catalytic materials (Zhao *et al.*, 1998). These materials have important applications in a wide variety of fields such as separation, catalysis, adsorption and advanced nanomaterials.

Mesoporous materials (SBA-15) are porous materials with pore diameters in the range of 2-50 nanometers (Xia *et al.*, 2003). SBA-15 is by far the largest pore size mesoporous material with highly ordered hexagonally arranged mesochannels, with thick walls, adjustable pore size from 3 to 30 nm, and high hydrothermal and thermal stability. SBA-15, which possesses larger pores, thicker walls and higher thermal

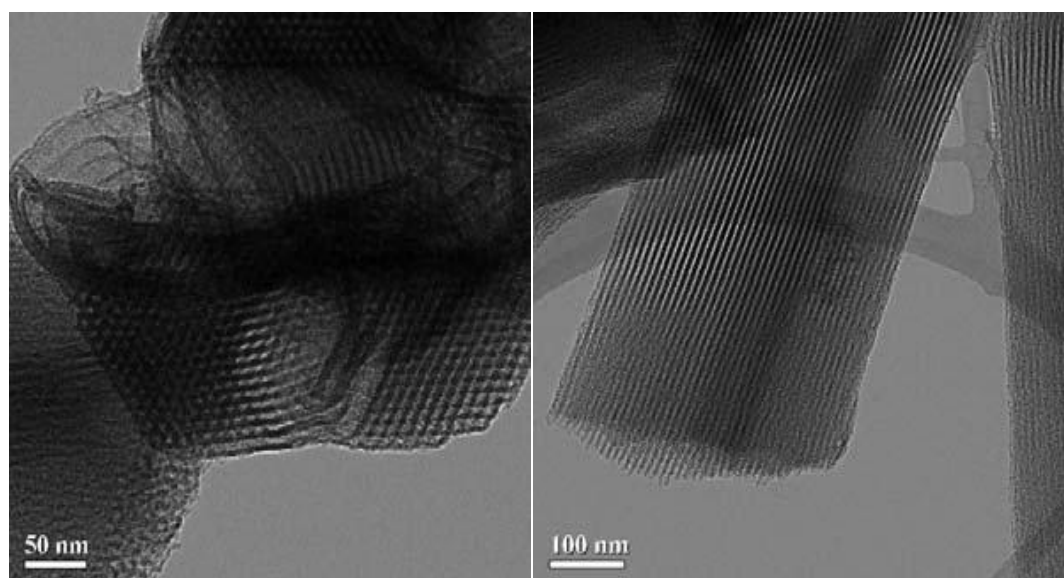
stability as compared other mesoporous silicas may be used a promising catalyst support, particularly for reactions occurring at high temperatures (Wang *et al.*, 2004).

Figure 2.1 shows the preparation of SBA-15 materials in a template process in acidic conditions with poly (alkaline oxide) tri-block co-polymers (Mukaddes, 2005). In acidic, aqueous solution, a structure directing agent (triblock copolymer of poly (ethylene oxide)-poly (propylene oxide)-poly (ethylene oxide)) is dissolved to form micelles. These block copolymers self-assemble to form unidirectional, cylindrical micelles in hexagonal arrays. Tetraethylorthosilicate (TEOS) is added to the solution, which polymerizes around the organic micelles forming the pore walls of the material. Finally, after filtration and washing, the material is calcined to combust the organic structure directing agent, leaving the mesoporous SBA-15 silica (Zhao *et al.*, 1998).



**Figure 2.1:** Synthesis of SBA-15 mesoporous silica (Mukaddes, 2005)

TEM result at Figure 2.2 showed the SBA-15 ordered structure of the material, and shows the cylindrical pores are arranged in an ordered hexagonal array (Akca, 2006). Recently, there are various studies carried out using SBA-15 as support. For example, SBA-15 supported  $\text{FePO}_4$  show higher  $\text{CH}_4$  conversion and HCHO selectivity than unsupported SBA-15 and MCM-41 supported one. The larger porous diameter and the 'inertness' of SBA-15 were probably responsible for the higher HCHO selectivity of the SBA-15 supported catalysts as compared with the MCM-41 supported ones particularly with low loading amount of  $\text{FePO}_4$  (Wang *et al.*, 2004).



**Figure 2.2:** TEM images of pure SBA-15(Akca, 2006)

In another study, by using SBA-15 supported iron (II)-bisimine pyridine catalyst was synthesized for ethylene polymerization. In polymerization, they found the supported catalyst can successfully control the morphology of polyethylene and the supported catalyst has fairly high catalytic activity for ethylene polymerization. (Akca, 2006).

As another example, impregnation of Co into MCM-41 and SBA-15 were implemented. It is observed that catalysts supported by SBA-15 are 5-10 times more active than supported by MCM-41. While MCM-41 structure collapsed after impregnation and BET surface area decreased with adding much amount of Co impregnation, SBA-15 structure led to no destruction of ordered structure (Mukaddes, 2005).

By adding noble metals or metal oxides, physical and chemical properties of mesoporous materials are improved (Mukaddes, 2005). However, it is very difficult to introduce the metal ions into SBA-15 directly due to the difficulties in the formation of metal –O–Si bonds under the strong acidic conditions for the synthesis of SBA-15 materials. Under strong acidic conditions, the metal ions will exist in the cationic form other than their corresponding oxo species (Mukaddes, 2005).

Notably, many efforts have been devoted to the incorporation of Al, Ti and V into SBA-15, including the two-steps pH adjusting methods (Li *et al.*, 2004), the hydrolysis-controlled methods ( Li *et al.*, 2004 and Zhang *et al.*, 2002) and microwave hydrothermal procedures (Chen *et al.*, 2004).

Mesoporous materials also have attracted significant attention in related fields of academia and industry, and have been widely applied as catalysts in petrochemical industry. However, the low acidity and hydrothermal stability limited their application in environmental catalysis, such as selective catalytic reduction (SCR) of NO in the presence of oxygen (Liang *et al.*, 2007). SBA-15 has adjustable pore diameter, thick pore wall and excellent hydrothermal stability. Therefore, it is probably appropriate to be used in SCR of NO with ammonia (Liang *et al.*, 2007).

### 2.3 Effect of Cobalt Loading

One important focus in the development of these catalysts is the improvement of the catalyst activity by increasing the number of active metal sites that are stable under reaction conditions. However, due to the strong interactions of cobalt species with the support more insight is needed into understanding the effect of the loading and size distribution on both the physico-chemical properties and performance of these catalysts (Tavasoli *et al.*, 2005). Surprisingly, there have limited studies have been reported in which systematically explored.

Iglesia *et al.* (1997) showed that the FT synthesis rates per total cobalt atoms increase linearly with increasing metal dispersion irrespective of the nature of the support used. In other words, the turnover rates are not influenced by support identity, and thus the catalyst activity should be proportional to the number of surface cobalt metal (Co) sites.

Jacobes *et al.* (2002) have shown that, increasing the cobalt loading, will improve the reducibility by decreasing the interactions with the support. By working at atmospheric pressure and differential conditions, Khodakov *et al.* (2007) observed an increase of the turnover rates by increasing the particle size of cobalt supported on mesoporous silicas of different pore size.

More recently Tavasoli *et al.* (2005) had done a research in addition of different loadings of Re and Ru to 15 wt % Co/Al<sub>2</sub>O<sub>3</sub> catalyst. The result has shown the final density of active Co sites depends on two main parameters, i.e., cobalt dispersion and the degree of reducibility of the supported oxidize cobalt species. Ideally, optimum cobalt catalysts should be prepared by achieving high dispersions of highly reducible cobalt species at cobalt loadings as high as possible. But due to high cost of cobalt, it is important to determine the appropriate loading of cobalt to maximize the availability of active cobalt surface sites for participation in the reaction, after catalyst activation.

## 2.4 Effect of Zinc Promoter

The goal of promotion is to enhance cobalt FT catalysts by the addition of small amount of noble metals and metal oxide. Numerous studies have shown that introduction of noble metals such as (Ru, Co, Zn, Pt, and Pd) has strong impact on the structure and dispersion of cobalt species. As example, analysis of the literature data suggest that introduction of noble metals could result on following phenomena (Khodakov, 2009):

- ❖ Ease cobalt reduction
- ❖ Enhancement of cobalt dispersion
- ❖ Better resistance to deactivation.
- ❖ Modification of intrinsic activity of surface site.

In order to gain access active site, noble metal promoters are often employed. These noble metal promoters, such as Pt or Ru, reduce at a lower temperature than the cobalt oxides, and catalyze cobalt reduction, presumably by hydrogen spill over from the promoter surface area (Wei *et al.*, 2001). However, the promotion with small amount of noble metal does not usually have noticeable effect on mechanical properties of cobalt supported catalysts (Wei *et al.*, 2001). Thus, addition of small amounts of noble metal only shifts the reduction temperature of cobalt oxides and cobalt species interacting with the support to lower temperatures (Wei *et al.*, 2001).

Due to the added expense of the promoter, it is important to determine the appropriate loading of promoter to maximize the availability of active cobalt surface sites for participation in the reaction, after catalyst activation.

Textural promoters, such as catalyst supports and support modifiers, are used typically to increase the dispersion of the clusters, improve attrition resistance, enhance sulphur tolerance, or electronically modify the active metal site (Hilmen *et al.*, 1996).

Numerous studies have shown that by using noble metals such Ru, Pt, and Pd are more explore by many researcher ,but by using zinc as promoter is a new development of promoter because the price are lower than other (Tavasoli *et al.*,2007).

#### 2.4.1 Cobalt Dispersion

The presence of noble metal can affect particle size of both cobalt oxide and metallic cobalt. Analysis data suggests that the promotion with noble metals primarily reduces the sizes of cobalt oxide particles in weakly interacting supports, *e.g.* silica. The increase in cobalt dispersion in the presence of platinum in silica supported catalysts was observed by Schanke *et al.* (1995). In that work, the extent of reduction in the monometallic and Pt-promoted cobalt catalysts was close to 90%. The improvement in catalytic activity on promotion with Pt was attributed to the enhancement in cobalt dispersion. Higher cobalt dispersion was also observed by Tsubaki *et al.* (2001) in Pt and Pd promoted cobalt silica supported catalysts. Mauldin *et al.* (2001) reported that rhenium promotion increased cobalt oxide dispersion during preparation of Co/TiO<sub>2</sub> supported catalysts.

Promotion with noble metals can also affect the sizes of cobalt metal particles in the reduced cobalt catalysts. Increase in the surface area of metallic cobalt was observed after promotion of 20% Co/Al<sub>2</sub>O<sub>3</sub> catalysts with Pt, Ir, Re, or Ru (Shannon *et al.*, 2007). The effect of promotion with platinum on cobalt dispersion in the reduced catalysts was rather significant with cobalt alumina supported catalysts (Chu *et al.*, 2007).

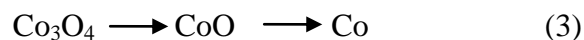
In contrast to silica supported counterparts, in alumina supported catalysts, promotion with Pt did not result in a decrease in the sizes of cobalt oxide particles in the calcined catalysts. At the same time, the average size of cobalt metallic particles was smaller in the catalysts promoted with Pt than in the monometallic counterparts.

Preliminary analysis indicated the presence of only single domain ferromagnetic cobalt particles in the catalysts.

#### 2.4.2 Cobalt Reducibility

Largely shown that promotion of cobalt catalyst FT process with noble metals also enhances cobalt reducibility. The improvements in cobalt reducibility may occur without any affect on cobalt dispersion as observed by Davis *et al.* (2005) for CoRe/Al<sub>2</sub>O<sub>3</sub> catalysts. While the improvement in cobalt reducibility has been observed with several noble metals as platinum, rhenium and ruthenium seems to be the most efficient cobalt reducibility promoters (Tsubaki *et al.*, 2001).

The effect of promotion with noble metals on cobalt reducibility is particularly pronounced with alumina supported catalysts. It was shown using XPS by showing the monometallic cobalt alumina-supported catalysts reduction with hydrogen, cobalt was almost exclusively in oxidized (CoO) form, while promotion with Pt resulted in a considerable fraction of metallic cobalt (Zsoldos *et al.*, 1991). It notes that even very small amounts of noble metals (0.05-0.1 wt %) are often sufficient for enhancement in cobalt reducibility. In the oxidic form of cobalt catalysts, Co<sub>3</sub>O<sub>4</sub> is usually the dominant cobalt phase. There have a suggestion that reduction of Co<sub>3</sub>O<sub>4</sub> to metallic cobalt may proceed via intermediate formation of CoO as mentioned on equation 3 (Khodakov *et al.*,1997):



Much easier reduction of cobalt in the presence of noble metals can be due to two different but complementary phenomena. First, it was shown that cobalt reduction proceeds via nucleation/growth autocatalytic model: once metal nuclei have formed on



the metal surface, they serve to facilitate the reduction process, most likely via the dissociation and spillover of hydrogen (Hilmen *et al.*,1996). It is known that noble metals can be easily reduced to the metallic state at much lower temperatures than cobalt oxide. At their metallic state, the noble metals would facilitate dissociation and activation of hydrogen and thus enhance the whole cobalt reduction process. This would decrease the temperature of appearance of cobalt metal phase.

The second mechanism of influence of noble metal on cobalt reduction involves formation of bimetallic particles of cobalt with noble metals. Because of incorporation of noble metal atoms in cobalt particles, these particles can be reduced at much lower temperatures than monometallic cobalt. In alumina supported Pt-supported catalysts Jacob *et al.*(2007) showed that Pt is likely to be situated on the edge of the cobalt metal cluster without forming Pt-Pt bonds.

It was suggested that reduction occurs on Pt first, allowing hydrogen to spill over to the cobalt oxide and nucleate cobalt metal sites. Note that nevertheless the spillover mechanism seems to be predominant in the cobalt catalysts promoted with noble metals, since cobalt reduction proceeds much more readily in the presence of noble metal when even no bimetallic cobalt particles have been detected.

### **2.4.3 Enhancement of Catalytic Performance**

A significant number of publications have addressed the effect of promotion with noble metals on the performance of cobalt catalyst. These effects depend on the catalyst synthesis and test conditions. The most noticeable effect is a considerable increase in the rate of carbon monoxide conversion rate at steady state conditions. The steady state conditions are usually attained after several hours or several days of FT synthesis. The magnitude of enhancement of catalytic performance depends however on the type of catalytic support, noble metal and reaction conditions. Noble metal

promotion of alumina-supported cobalt catalysts is known to produce the most active cobalt catalysts for FT synthesis (Khodakov *et al.*, 2009)

The effect of promotion with noble metals on FT catalytic performance is usually less pronounced with silica and titania supported catalysts. Many researcher observed about catalytic performance with various condition of promoter ,supported and any condition that influence the performance of FT. Storaester *et al.*(2007) evaluated the catalytic performance of different cobalt supported catalysts in a fixed bed reactor and the monometallic catalysts exhibited hydrocarbon conversion rates between 0.14 and 0.25 gHC/(gcat h). Promotion with Re resulted in a double increase in the rate of hydrocarbon production, while methane and C<sup>5+</sup> selectivities were not much affected.

Thus, promotion of cobalt catalysts with noble metals usually results in a considerable increase in overall FT reaction rate which is accompanied by a much smaller effect of the promotion on hydrocarbon selectivity. Higher promoter content can favor methanation, affect chain growth probability and lead to a much lower the selectivity to higher hydrocarbons. Note that these phenomena represent a general trend observed in the literature about FT catalysts. It should be emphasized however that the catalytic performance of cobalt FT catalysts is very sensitive to catalyst preparation and conditions of catalyst evaluation. Some additional effects of noble metals on the catalytic performance of cobalt FT catalysts can be observed as a function of catalyst preparation, activation and testing conditions.

## **2.5 Ways for the Impregnation/Incorporation of Metal on the Catalysts**

Mesoporous silica materials are not catalytically active by themselves. These materials have to be functionalized in some way for application as catalysts. Review from Akca. (2006) there are several procedures that are applied to functionalize catalysts and two of the most commonly used for mesoporous materials are direct

functionalization by metal incorporation and incipient wetness impregnation (Taguchi *et al.*, 2005).

The direct method is a “one-pot” procedure, where the metal precursors are added during synthesis and are incorporated into the framework. This one-step procedure is relatively simple, and it is also possible to control the pore size, pore structure, and metal amount during synthesis. However, the framework becomes less thermally stable due to the incorporated metals (Tuel, 1999). Since the wall thickness of mesoporous materials is about 1 nm, a significant portion of the incorporated metals will be located inside the walls and thus inaccessible as catalytically active sites. Incipient wetness impregnation is a widely used functionalization method for preparation of supported catalysts and is also applied industrially.

In this post synthesis procedure, a metal salt solution is added to the support in an amount to exactly fill the pore volume, and the material is then dried and calcined (Perego *et al.*, 1997). This procedure is simple; however, a large portion of the precipitated particles ends up outside the pore system of the support. Some of the advantages of having a mesoporous support with an ordered and well-defined pore structure may therefore be lost if the active particles are located at the external surface. Incipient wetness impregnation may therefore not be so suited for functionalization of mesoporous materials, at least not for model studies.

While the direct method typically will result in a relatively homogeneous incorporation of the heteroelement, post-synthesis treatment will primarily modify the wall surface and thus lead to increased concentration of the heteroelement on the surface (Taguchi *et al.*, 2005).

The possible pathways to modify mesoporous materials to give them a new catalytic function are schematically shown in Figure 2.3.

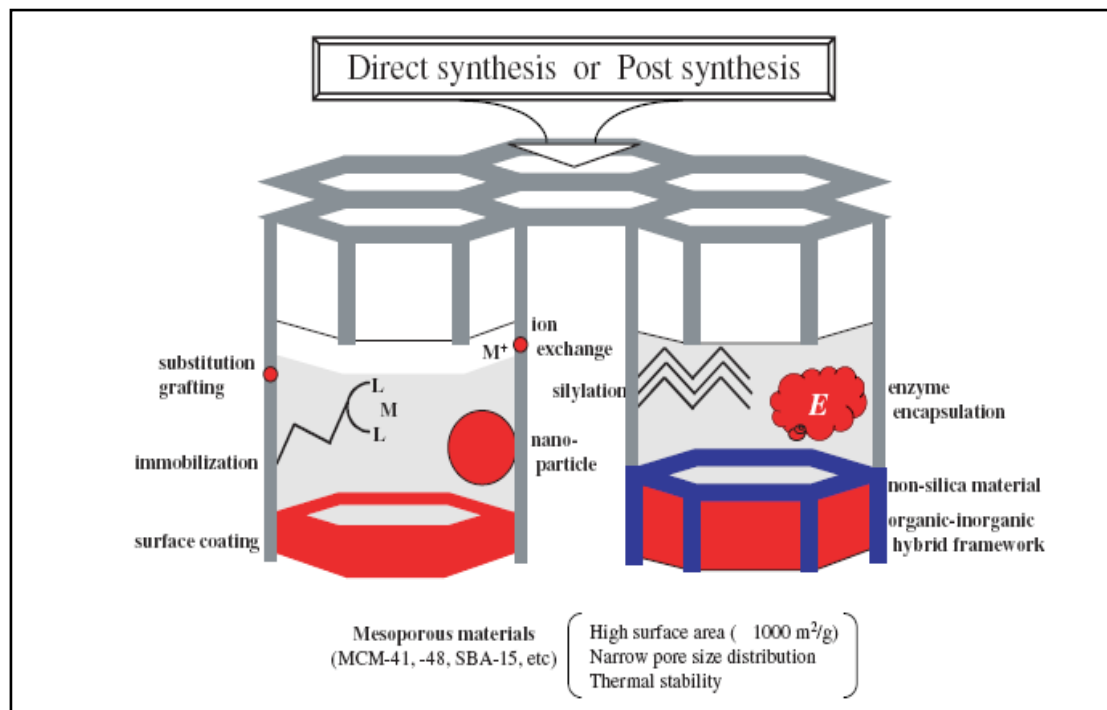


**Figure 2.3** Schematic sketches of the various methods for the functionalization of mesoporous material (Taguchi *et al.*, 2005)

In order to modify the catalytic activity of the mesoporous materials, especially to create active sites, several other metal ions were incorporated into the silica framework or grafted on the surface (titanium, zirconium, iron, cobalt, zinc, platinum, etc). Compared to other support materials, the ordered mesoporous solids have the advantage of stabilizing metal or metal oxide particles, since they cannot grow to sizes larger than the pore size unless they move to the external surface of the particles (Taguchi *et al.*, 2005).

Even though many applications do not require high temperatures, the hydrothermal stability of the catalyst is still critical for such classical catalytic processes as cracking or hydrotreatment. Hydrolysis of the Si–O–Si bridges leads to the pore lattice collapse. Therefore, structural stability is dependent on the level of condensation in walls (related to wall thickness) and to the surface density of silanol groups. This explains why thicker wall materials such as those synthesized using triblock copolymers

as surfactants, exemplified by SBA-15, are more stable than M-41S solids (Akca, 2006).

## **2.6 Catalyst Characterization.**

### **2.6.1 Thermogravimetric Analysis (TGA)**

Basically, Thermo gravimetric Analysis (TGA) is the equipment for measures weight changes in a material as a function of temperature (or time) under a controlled atmosphere. Its principal uses include measurement of a material's thermal stability and composition. TGA instruments are routinely used in all phases of research, quality control and production operations. A simplified explanation of a TGA sample evaluation may be described as follows. A sample is placed into a tarred TGA sample pan which is attached to a sensitive microbalance assembly. The sample holder portion of the TGA balance assembly is subsequently placed into a high temperature furnace. The balance assembly measures the initial sample weight at room temperature and then continuously monitors changes in sample weight (losses or gains) as heat is applied to the sample. Typical weight loss profiles are analyzed for the amount or percent of weight loss at any given temperature. Figure 2.4 show the example of collected data for TGA analysis for SBA-15.

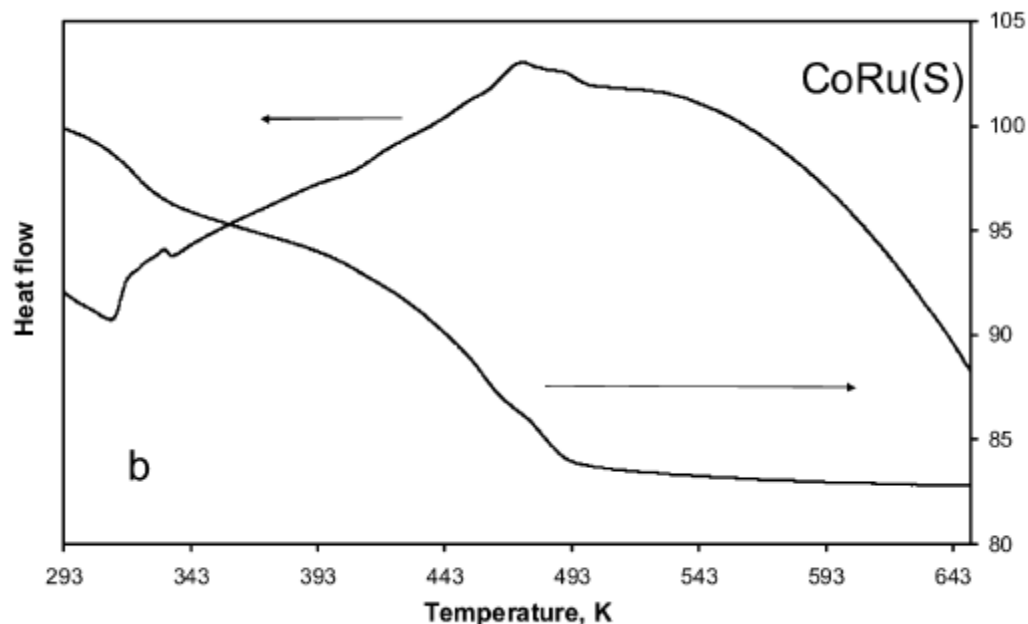


**Figure 2.4:** DSC-TGA curves of cobalt silica-supported catalysts promoted with Re and Ru and prepared without and with addition of sucrose.

Temperature ramp 1 K/min (Girardon *et al.*, 2007)

The DSC-TGA curves of the catalysts prepared from cobalt nitrate promoted with ruthenium and rhenium and with the addition of sucrose are shown in Figure. 2.4. All of the DSC-TGA curves were measured in air flow. The decomposition profiles for the CoRu and CoRe catalysts are similar and resemble the DSC-TGA curves of unpromoted cobalt silica supported catalysts. Two endothermic weight losses (6.7–7.6%) are observed at 323–328 and 363–364 K. These losses can be attributed to the dehydration of cobalt nitrate and silica. An additional weight loss (10.4–11.7%) was detected at 431–432 K, attributed to the decomposition of  $\text{NO}_3$  groups. As with monometallic cobalt catalysts, for all promoted catalysts, the total experimental weight loss is much smaller than the theoretical one calculated from decomposition of supported bulk cobalt nitrate to  $\text{Co}_3\text{O}_4$  (29%). This difference can be explained in terms of lower extent of hydration and partial decomposition of cobalt nitrate before calcinations.

### 2.6.2 N<sub>2</sub> Adsorption Analysis.

Gas adsorption, particularly nitrogen or argon adsorption, is one of the most powerful technique for characterization of porous materials and can provide a lot of useful information about adsorbent's surface area and structural properties. Adsorption analysis can provide such data as the specific total pore volume, BET specific surface area and pores size distribution of porous materials in the case of structural properties. Commonly, from the data collected the dispersion of metal oxide to the support of catalysts can be determined. For example, the below data collected show the decreasing of total pore volume due to increasing of cobalt contents, it is shown that the dispersion of cobalt to catalysts support in increase, and higher dispersion to catalysts results on blocking the pore of the catalyst.

**Table 2.1:** Chemical composition and textural properties obtained from N<sub>2</sub> adsorption isotherms of SBA-15-supported Co catalysts  
(Martinez *et al.*, 2003)

Chemical composition and textural properties obtained from N <sub>2</sub> adsorption isotherms of SBA-15-supported Co catalysts					
Catalyst	Co (wt%)	Promoters (wt%)		S <sub>BET</sub> (m <sup>2</sup> /g)	Total pore volume (cm <sup>3</sup> /g)
		Re	Mn		
SBA-15	–	–	–	842	1.18
10CoSBA-n	9.2	–	–	607	0.83
20CoSBA-n	18.0	–	–	508	0.62
30CoSBA-n	28.7	–	–	421	0.60
40CoSBA-n	40.8	–	–	350	0.49
20CoSBA-ac	17.5	–	–	467	0.62
20CoSBA-aa	16.4	–	–	355	0.55
1Re20CoSBA-n	17.9	0.9	–	498	0.74
2Mn20CoSBA-n	17.8	–	1.8	476	0.76
1Re2Mn20CoSBA-n	17.9	1.3	2.0	443	0.63
20CoSiO <sub>2</sub>	20.5	–	–	262	0.60

The data observed from the Table 2.1 showed the BET surface area of the Re and Mn promoted samples was similar to that of the unpromoted catalyst with comparable Co loading. The chemical composition and textural properties obtained by  $N_2$  Adsorption of pure silica SBA-15 sample and supported cobalt catalyst are given in table 2.3. The BET surface area and total pore volume of the siliceous calcined SBA-15 (842  $m^2/g$  and 1.18  $cm^3/g$ , respectively) are typical for siliceous SBA-15 synthesized under similar conditions. Both the BET surface area and the total pore volume significantly decreased upon Co impregnation, with the decrease higher at larger Co loading. This may be caused by a partial blockage of the SBA-15 pores by cobalt oxide clusters and/or a partial collapse of the mesoporous structure

### 2.6.3 Fourier Transform Infrared (FTIR)

FTIR stands for Fourier Transform Infrared, the preferred method of infrared spectroscopy. In infrared spectroscopy, IR radiation is passed through a sample. Some of the infrared radiation is absorbed by the sample and some of it is passed through (transmitted). The resulting spectrum represents the molecular absorption and transmission, creating a molecular fingerprint of the sample. For most common material, the spectrum of unknown can be identified by comparison to library of known compounds. To identify less common materials, FTIR will need to be combined with nuclear magnetic resonance, mass spectrometry, emission spectroscopy, and X-ray diffraction. Figure 2.5 show the example of collected data. Information listed below is the function of FTIR provided.

- ❖ It can identify unknown materials.
- ❖ It can determine the quality or consistency of a sample.
- ❖ It can determine the amount of components in a mixture.



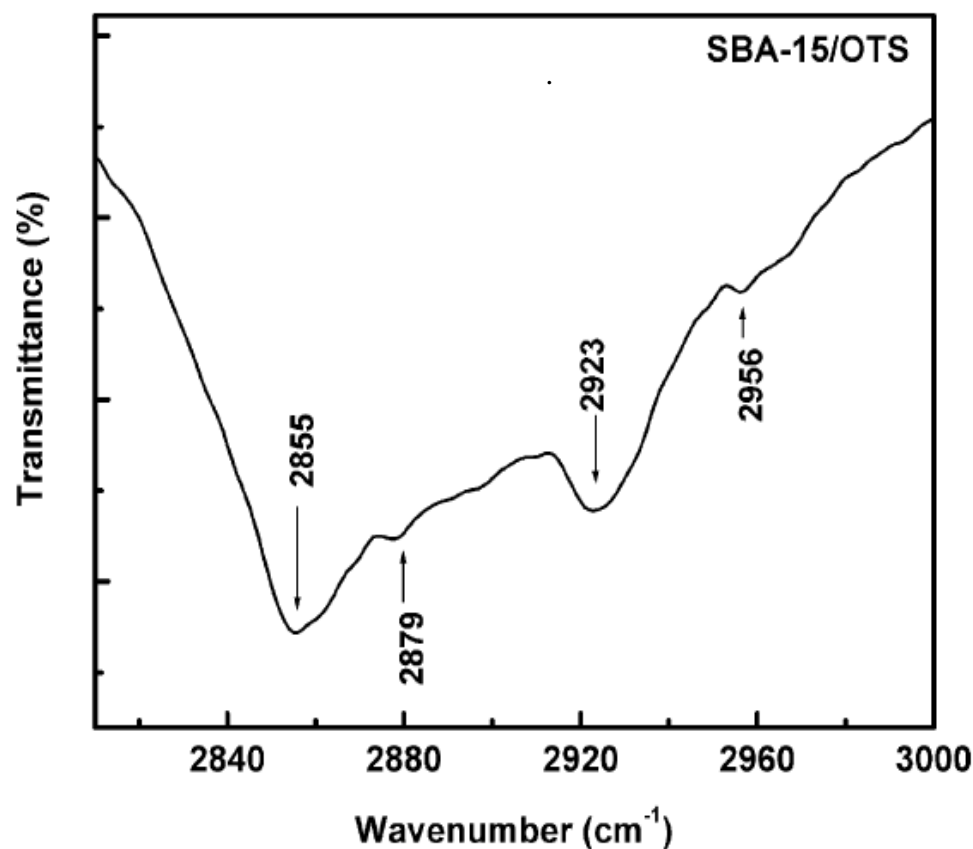


**Fig. 2.5:** FTIR spectra in the C–H stretching region of SBA-15 with OTS adsorption showing –CH<sub>2</sub> and –CH<sub>3</sub> stretching bands

(Mirji *et al.*, 2006)

From the figure given, the result show FTIR spectra in the C–H stretching region of SBA-15 after OTS adsorption, methylene (–CH<sub>2</sub>) and methyl (–CH<sub>3</sub>) asymmetric and symmetric C–H bands are observed. These observations clearly suggest OTS adsorption are highly ordered, densely packed OTS monolayer with close to perpendicular chain axis orientation has a methylene (–CH<sub>2</sub>) asymmetric and symmetric stretching at 2920 cm<sup>-1</sup> and 2850 cm<sup>-1</sup>. Respectively, methyl (–CH<sub>3</sub>) asymmetric and symmetric stretching at 2968 and 2879 cm<sup>-1</sup>. Respectively, CH<sub>2</sub> asymmetric and symmetric stretching observed for OTS on SBA-15 are 2923 and 2855 cm<sup>-1</sup>. Respectively, CH<sub>3</sub> asymmetric and symmetric stretching observed are at 2956 and 2879 cm<sup>-1</sup>, respectively. The intensity ratio of (–CH<sub>3</sub>) to (–CH<sub>2</sub>) vibrations indicate the orientation of alkyl chain relative to the surface.

## 2.6.4 Scanning Electron Microscopy (SEM)

Scanning electron microscopy analyses are used to determine the surface morphology of catalyst such as a shape, size and crystallinity of the catalyst. Figure 2.6 show the example of SEM micrograph.

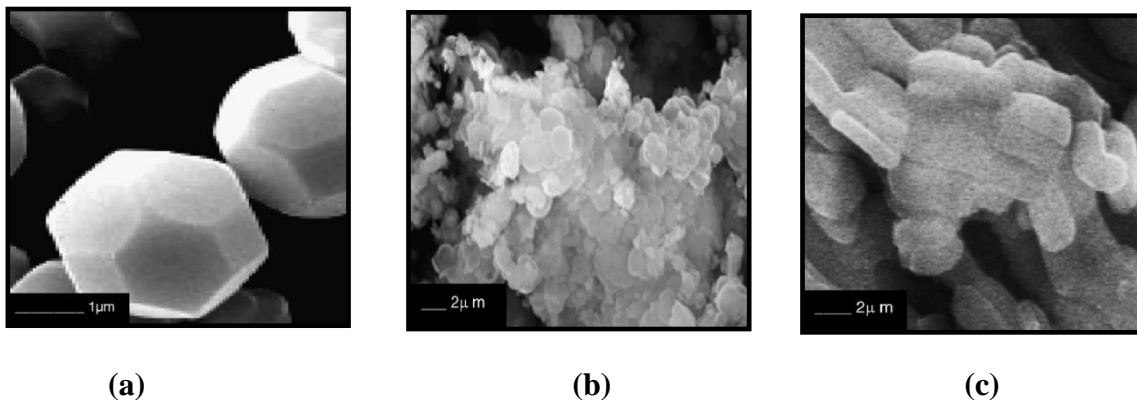


**Figure 2.6:** SEM microphotographs of (a) SBA-1,(b) SBA-3, and (c) SBA-15(Anunziata *et al.*, 2007)

The size and shape of the samples indicate good morphology of the crystals, without other phases, and typical of these materials. The images were shown in Figures 2.6a–2.6c. As shown in 2.6, separated almost spherical or spheroid crystals but have glass-like disorder in the walls observed for SBA-1 sample. The particle size of the siliceous SBA-1 was 1.5–2.2 μm in diameter, whereas for SBA-3 the crystal form was almost spherulitic with lower crystal size (0.8–1.3 μm). SBA-15 images reveal that it consists of many rope-like domains with relatively uniform sizes of 1.5–2 μm, which are aggregated into wheat-like macrostructures.

## CHAPTER 3

### MATERIAL AND METHODOLOGY

#### 3.1 Introduction

The experiment techniques used for the preparation and characterization of the support and the catalyst through this research are summarized and presented in this chapter. The overall experimental works are summarized in the Figure 3.1 below.

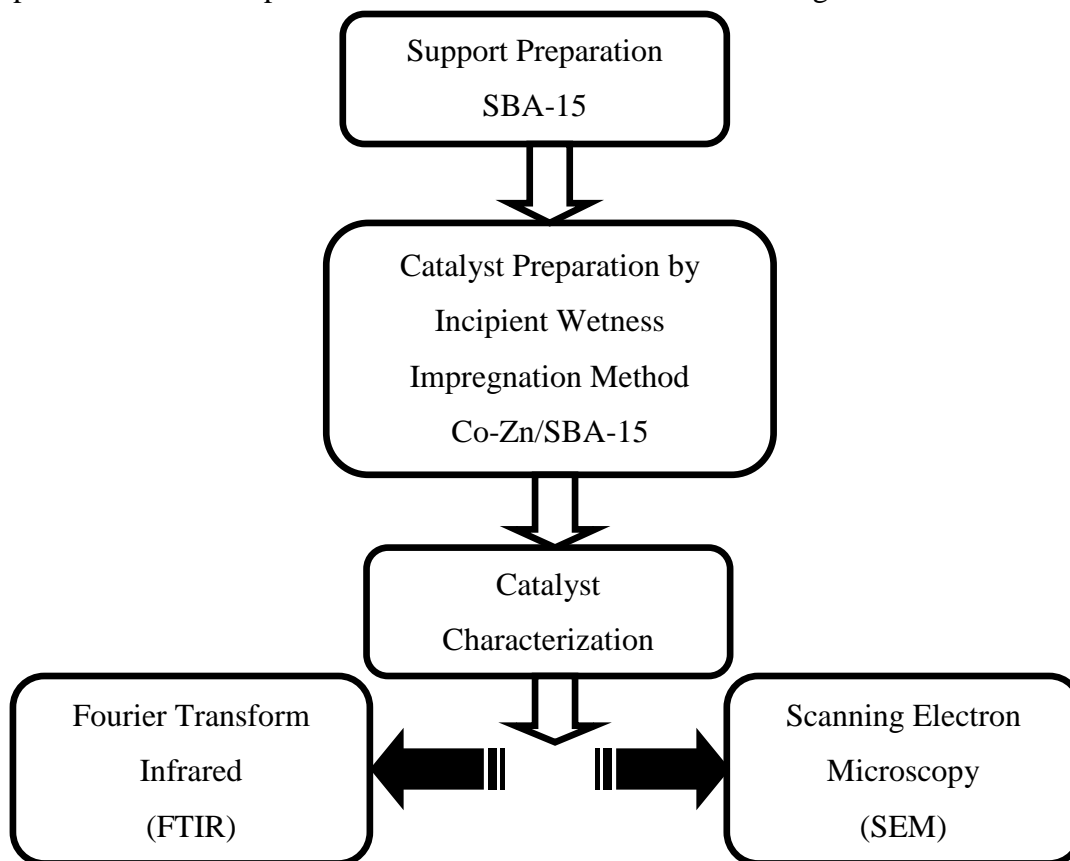


**Figure 3.1** Flow chart of overall experimental work.

### 3.2 Materials and Chemicals

All chemicals and materials used in the present study are listed as Table 3.1 below:

**Table 3.1** List of Chemicals

Chemical	Molecular Formula	Supplier	Purity %
Cobalt Nitrate	$\text{Co}(\text{NO}_3)_2 \cdot 6\text{H}_2\text{O}$	Merck	99.0 %
Zinc Nitrate	$\text{Zn}(\text{NO}_3)_2 \cdot 6\text{H}_2\text{O}$	R&M Chemical	-
Pluronic P-123	$\text{HO}(\text{CH}_2\text{CH}_2\text{O})_{20}(\text{CH}_2\text{CH}(\text{CH}_3)\text{O})_{70}\text{H}$	Aldrich	-
Acid hydrochloric	HCl	UMP Sources	37%
TEOS tetraethylorthosilicate	$(\text{Si}(\text{OCH}_3)_4)$	Merck	>9%

### 3.3 SBA-15 Preparations

150 ml HCl with concentration of 2M was shaken in orbital shaker at 40°C for an hour. 4g pluronic P123, triblock copolymer was then dissolved in the HCl solution and the mixture was shaken at 40°C for an hour. 9 ml of tetraethyl orthosilicate (TEOS) were added to the above solution. The mixture was stirred for 2 hours. As the gel started to develop the mixture was heated at 40°C under slow shaking at 50 rpm for 24 hours. Then the solid formed was vacuum filtered, washed several time with distilled water calcined at 500°C for 6 hours in furnace.

### 3.4 Co-Zn /SBA-15 Synthesis

Co-Zn/SBA-15 with same zinc content (20 wt %) and different cobalt content with range between 5 wt% until 15 wt% were prepared by incipient wetness impregnation of SBA-15 where the weight percent of cobalt and zinc loading was determined by calculate the amount of cobalt nitrate and zinc nitrate desired. The catalyst, then were dried overnight in an oven at 60°C and calcined at 500°C for 6 hours. The Co catalyst with the addition of zinc promoter will label as *x* Co-Zn/SBA-15 with *x* standing for cobalt weight percent in the samples. The calculations are summarized in Table 3.2 and the detail calculations are shown in Appendix A1.

**Table 3.2** Percentage of metal loading in the SBA-15

<b>Sample</b>	<b>5Co-Zn/SBA-15</b>	<b>10Co-Zn/SBA-15</b>	<b>15Co-Zn/SBA15</b>
<b>Ratio Co: Zn (% wt)</b>	5:20	10:20	15:20
<b>Weight Co(NO<sub>3</sub>)<sub>2</sub> (g)</b>	0.328	0.9766	2.863
<b>Weight Zn(NO<sub>3</sub>)<sub>2</sub> (g)</b>	10.25	10.25	10.25

### 3.5 Catalyst Characterization

All samples were subjected to comprehensive characterization tests, depending on types of data to be obtained. The data that collected was used as references between

pure SBA-15 and modified Co-Zn/SBA-15 catalyst. The samples were characterized using Fourier Transmitter Infrared Analysis (FTIR) and Scanning Electron Microscope (SEM) in order to obtain their physicochemical properties.

### **3.5.1 Fourier Transmitter Infrared Analysis (FTIR)**

FTIR Analysis is an analysis technique that provides information about the functional group of materials, whether organic or inorganic. The resulting FTIR spectral pattern was then analyzed and matched with known signatures of identified materials in the FTIR library. The FTIR analysis was conducted at FKKSA Analytical Lab Unit, Universiti Malaysia Pahang Gambang.

### **3.5.2 Scanning Electron Microscope (SEM)**

Scanning electron microscopy (SEM) enables one to study a crystal's topography. SEM images were obtained for the synthesized SBA-15 samples using a JEOL JEM-5400 scanning electron microscope. The micrograph shows the particle size and its morphology. However, a morphological study is beyond the scope of this work and therefore will not be discussed in detail. The analysis was conducted at Faculty of Science Technology & Industry Lab Unit, Universiti Malaysia Pahang Gambang.

## CHAPTER 4

### RESULTS & DISCUSSIONS

#### 4.1 Scanning Electron Microscopy (SEM)

Scanning electron microscopy (SEM) has been used to study on the surface morphology of structure of SBA-15 and modified catalyst by noble metal. The SEM images of mesoporous SBA-15 particles before and after surface modification by Co loading and Zn loading are shown in Figure 4.1 (a) and (b).

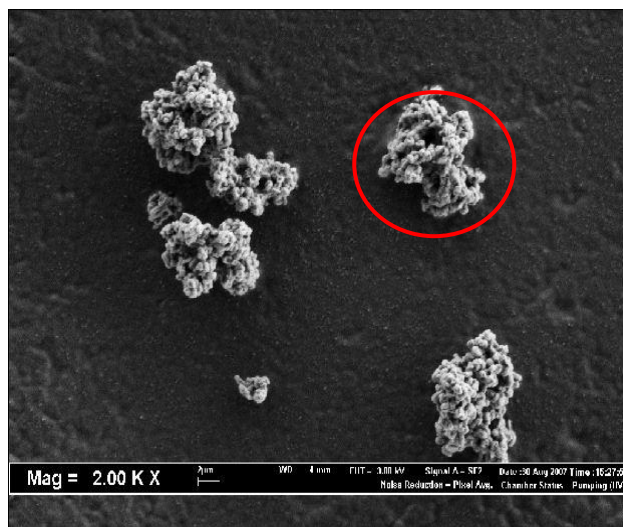


**Figure 4.1 (a)** SEM microphotograph of SBA-15

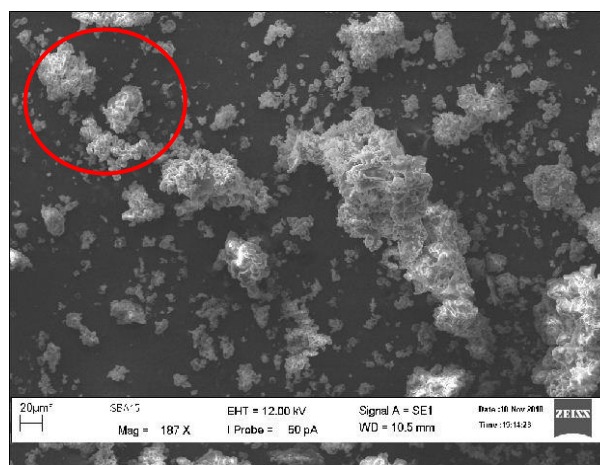


**Figure 4.1(b)** SEM microphotograph of 15%Co-20%Zn/SBA-15

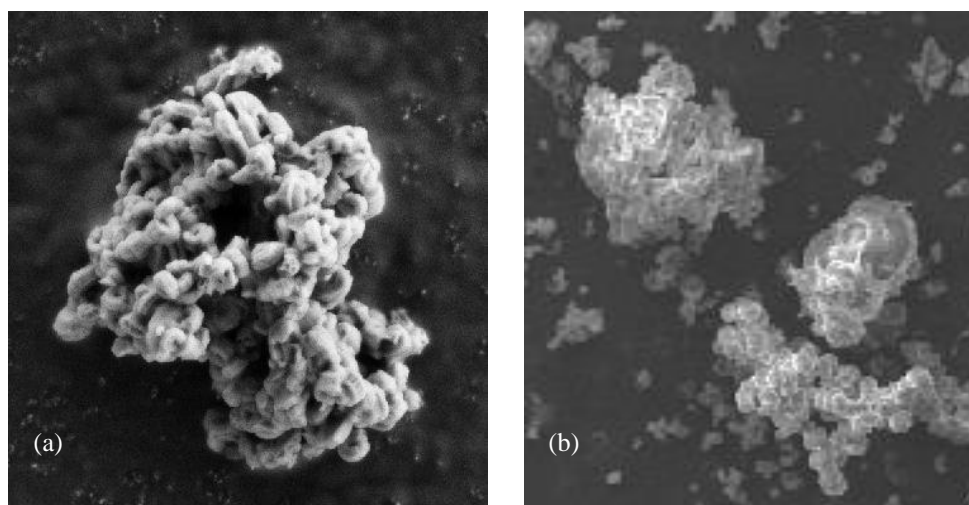


**Figure 4.1:** SEM monograph of mesoporous: (a) SBA-15 (b) Co-Zn/SBA-15.  
(Magnification)

Respectively, the SBA-15 reveal that it consists of many rope-like domains with relatively uniform sizes of 1.5-2  $\mu\text{m}$ , which are aggregated into wheat-like macrostructures mean that rod-like primary particles aggregated to form micron-sized fibers. This result finding same with Anunziata *et al.* (2007) mentioned.



The form of SBA-15 also exhibits irregular spherical shape and are clearly visible in agglomeration and homogeneous formed. Recently, Mirji *et al.* (2006) mentioned the same observation that reveal the spherical shape with agglomeration and homogenous. The form shown clearly visible. After modification of SBA-15 by Co loading and Zn loading, the particles found to be attached closely with each other. The SEM picture in Fig. 4.1b clearly shows a large number of SBA-15 particles attaching closely with one another. These phenomena observed both in microscopic and macroscopic scale could be due to spine (alkyl chain) like Co and Zn growth on SBA-15 (Mirji *et al.*, 2006). These spines of one SBA-15 particle may be caught on the spine of another SBA-15. This way the bonding of large number of SBA-15 particles may take place. On the other hand, it could be due to van der Waals and electrostatic interaction of alkyl chains between the Co and Zn of adjacent SBA-15 particles (Mirji *et al.*, 2006). Nevertheless, the good morphology is obtained (Anunziata *et al.*, 2007).

## 4.2 Fourier Transform Infrared (FTIR)

Figure 4.2 show the selected FTIR spectra. All support and catalyst samples were analysed using FTIR spectra to investigate the existence of functional groups formed in the samples and provide surface information of materials for identification of chemical groups. Figure 4.2 shown four curves of SBA-15 sample, Co (5 wt%)-Zn (20 wt %) /SBA-15, Co (10wt%)-Zn (20 wt %) /SBA-15, and Co (15wt%)-Zn (20wt %) /SBA-15. There are many functional groups observed with certain wavelength in the samples such as cobalt oxides, Si-O-Si, Si-OH, zinc oxide, OH band, nitrate group, and etc.

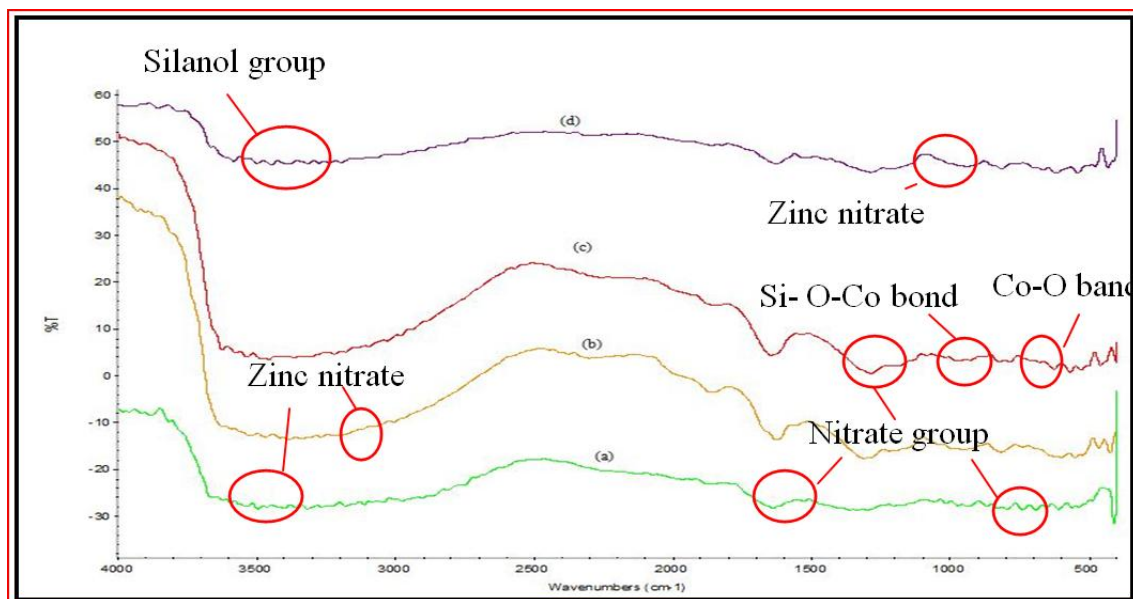


**Figure 4.2:** FT-IR spectra of (a) SBA-15 (b) Co (10wt%)-Zn (20wt %) /SBA-15 (c) Co (15wt %) Zn (20wt %) /SBA-15 (d) Co (5wt%)-Zn (20wt %) /SBA-15

In this research, the sample of SBA-15 and SBA-15 modified by adding cobalt nitrate and zinc nitrate are formed. When comparing the curve of SBA-15 with curve of  $x$  wt% Co-Zn/SBA-15 ( $x=5, 10, 15$ ), the significant changes were analysed at any peak showed in Figure 4.2. Firstly, the changes on SBA-15 curve showed that SBA-15 consist of OH bond stretching's Si-O-Si and Si-OH. The O-H bond stretching bands of the silanol groups of SBA-15 are observed at  $3200-3600\text{ cm}^{-1}$ . Silanol groups on the silica surface exist in several forms such as isolated, hydrogen-bonded, and geminal types of silanol groups, IR absorption bands of which correspond to the peaks at  $3738\text{ cm}^{-1}$  and  $3200-3600\text{ cm}^{-1}$  (Akca *et al.*,2008). The results show that the surface silanol group of unmodified SBA-15 is mainly of the hydrogen-bonded type in IR absorption bands, which absorb at  $3200-3600\text{ cm}^{-1}$  (Akca *et al.*,2008). The siloxane or Si-O stretching bands, peak appears as a broad and strong peak in the range  $1000-1200\text{ cm}^{-1}$  (centered at  $1100\text{ cm}^{-1}$ ). The Si-O stretching band is clearly visible at band  $1100\text{ cm}^{-1}$  (Akca *et al.*, 2008).

Furthermore, formation of hydroxyl group also formed when SBA-15 are present in the sample. The hydroxyl groups were assigned around  $1640\text{ cm}^{-1}$  (Kababji *et al.*, 2009). The sample on spectrum (a) and (d) contains more hydroxyl groups (SiOH) than the other samples that mean the spectrum shows higher intensity of the bands when comparing to the other spectrum. The higher amount of SiOH groups in spectrum (a) and (d) probably favors the formation of higher amount of tetrahedrally coordinated  $\text{Co}^{2+}$  ions, interacting with the silica support. When the silica support is impregnated by an ionic solution, the adsorption of ions is strongly affected by the surface charge of the support (Agnes *et al.*, 2009). The existence of silanol group (SiOH) on the silica surfaces also plays an important role in the formation of cobalt species (Kababji *et al.*, 2009). As the modified of surface silanol groups of SBA-15 by increasing the cobalt loading, the density of the surface silanol groups decreases. Therefore, the O–H bond stretching bands of silanol groups decrease (Agnes *et al.*, 2009).

Interestingly, sample SBA-15 does not show any nitrate ion peak absorbencies because no nitrate group was added while conducting experiment. But for another sample, there is shown a peak represent nitrate group. This is due to a possible interaction between hydrate silica in the higher surface area of each sample and the nitrate ion during preparation (Kababji *et al.*, 2009). All spectrum confirms the absorbance of nitrate group ( $1610, 1365, 842\text{ cm}^{-1}$ ) indicating the existence of some cobalt nitrate residue due to low drying temperature.

Furthermore, FTIR spectrum also shows zinc nitrate  $\text{Zn}(\text{NO}_3)_2 \cdot 6\text{H}_2\text{O}$ , the components of zinc nitrate are attended at OH stretching vibration area. The region of OH stretching vibrations contains three major absorption bands, at  $3536, 3483,$  and  $3184\text{ cm}^{-1}$ , in accordance with the presence of different OH environments as evidence from the structural data (Eriksson *et al.*, 1989). The broad band centred at  $3184\text{ cm}^{-1}$  may be assigned to OH vibrations of water molecules whereas the bands at  $3536$  and  $3483\text{ cm}^{-1}$  may be assigned to OH vibrations of the layer hydroxyls.

The presence of structural water in this material is confirmed by the appearance of the H<sub>2</sub>O bending vibration at 1664 cm<sup>-1</sup> ( Biswick *et al.*, 2007). In zinc nitrate the characteristic set of stretching vibrations attributed to nitrate anion appears at 1420, 1338 and 1050 cm<sup>-1</sup> and are assigned to the asymmetric stretch ,the symmetric stretch and the N–O stretch respectively (Biswick *et al.*, 2007).

Indicating the existence of cobalt nitrate residue, the presence of spinel Co-O bond absorbance peak corresponding to Co<sub>3</sub>O<sub>4</sub> is clearly visible around 667 cm<sup>-1</sup>. Another weak Co-O absorbance peak exist around 580 cm<sup>-1</sup> probably due to a small amount of Co-O formation (Kababji *et al.*,2009). The small amount of Co-O are explained by possible oxidative aggregation of CoO to a large cluster Co<sub>3</sub>O<sub>3</sub>.

Figure 4.2 represents the pure SBA-15 sample which has similar IR features as sample Co(5%)-Zn(20%)/SBA-15 as well as the other catalyst samples prepared but with different peak intensities ( Kababji *et al.*,2009). It is also observed that the ratio of Co<sub>3</sub>O<sub>4</sub> to Si-O silica stretching peak intensity in spectrum (d) are less than the ratio of Co<sub>3</sub>O<sub>4</sub> peak to silica comparing with spectrum (a) (b) (c). The spectrum (c) observed that the highest ratio of Co<sub>3</sub>O<sub>4</sub> to Si-O silica stretching peak intensity .this leads to the conclusion that the lower surface area samples (d) contained more desired cobalt oxide species than other samples ( Kababji *et al.*,2009).

As expected, the absorption peaks of Co<sub>3</sub>O<sub>4</sub> are confirmed around 667 cm<sup>-1</sup> and 580 cm<sup>-1</sup>. The spectra of other samples were essentially the same but with different peak intensities. The spectrum (b) (c) (d) of catalyst with increasing cobalt loading and maintain zinc loading confirmed showed the effect of surface area on the resultant cobalt species formed on the support surface (Kababji *et al.*,2009).

While  $\text{Co}_3\text{O}_4$  is confirmed on the surface by Co-O vibration band at  $667\text{cm}^{-1}$ , it is also noticed that the broad absorbance peak Si-O ( $1100\text{ cm}^{-1}$ ) has disappeared and new broad peak around ( $1020\text{-}1080\text{ cm}^{-1}$ ) assigned to Si-O-Co bond has formed. This is the characteristic assigned to cobalt silicate (Puskas *et al*, 1992). The high support surface area enhanced the interaction of silica and the cobalt cations during the initial decomposition of cobalt nitrate precursor upon mixing in the presence of water. This resulted in the formation of aqueous cobalt complexes as well as attraction of less cobalts ion to the pores.

Upon drying and calcination, less cobalt oxides was formed as evident comparing the ratio of silica to cobalt oxide absorbance peaks in both spectra (b) and (c). this form are predicted by Puskas *et al*. (2007) where they found using infrared spectroscopy much less than expected  $\text{Co}_3\text{O}_4$  formation upon calcination when silica was used as a support explained that by reaction between CoO and  $\text{SiO}_2$  during calcination which prevented large amounts of CoO from further oxidation to form  $\text{Co}_3\text{O}_4$ .

## CHAPTER 5

### CONCLUSION & RECOMMENDATIONS

#### 5.1 Conclusion

In the first part of this thesis, the synthesis of SBA-15 as support for FT process had been achieved according to the procedure reported. Besides, Co and Zn incorporated SBA-15 mesoporous materials were synthesized by incipient wetness impregnation method by using cobalt nitrate as cobalt source and zinc nitrate as zinc source. The results for FTIR were identification of Si-O-Zn and Si-O-Co functional group because of the present of zinc or cobalt onto silica SBA-15 support at band  $1200\text{ cm}^{-1}$ . Besides that, the identification of metal inside SBA-15 was determined by comparing the pure SBA-15 with the incorporated metal on SBA-15. Last but not least when the preparation of 15 wt % of cobalt loading showed a more OH group were presented. For SEM analysis the rope like domain aggregated to wheat like microstructure were observed in the morphology of modified catalyst and SBA-15. The SEM results showed that incorporation of Co and Zn did not change the morphology of the support. For this research, the characterization of the catalyst by selecting Zn as promoter have quiet similar characterization with noble metal that already investigate.

## 5.2 Recommendations

As a recommendation for future improvement related to our research, research should be performed by using various data analysis to get better and persistent results. By using many characterization equipment such as thermo gravimetric analysis (TGA), X-ray diffraction analysis (XRD), N<sub>2</sub> Adsorption analysis, transmission electron microscopy analysis (TEM), we can know deeply about the characteristics of our samples. By using all the characterization equipment above, many information about thermal stability, cobalt dispersion on SBA-15 based on pore volume, BET surface area, cobalt surface density and give information about crystal structure of a sample.

Furthermore, improvement of our research also can be better when we further by performing catalytic activity of FT reaction by using the catalyst. From the reaction condition, we will know the catalyst activity and the stability of catalyst is possible or impossible to use for FT industry. Besides, by performing regeneration of catalyst also can give improvement for our research.

## REFERENCES

- Agnes Szegedi., Margarita Popova and Christo Minchev, “Catalytic Activity of Co/MCM-41 and Co/SBA-15 Materials in Toluene Oxidation”, *J Mater Sci*, 44, 6710 – 6716 (2009).
- Akca B., “Synthesis and Characterization of Co-Pb/SBA-15 Mesoporous Catalysts”, *Master Thesis*, Graduate School of Natural and Applied Science of Middle East Technical University (2006).
- Andrei Y Khodakov, “Fisher Tropsch Synthesis: Relation between of Cobalt Catalysts and their Catalytic Performance”, *Catalysis Today*, 144, 251-257 (2009).
- Anunziata O. A., Andrea R .Beltmone, Maria L. Martinez and Lizandra Lopez Belon, “Synthesis and Characterization of SBA-1,SBA-15 and SBA-3 Nanostructure Catalytic Materials”, *Journal Of Colloid and Interface Science*, 315, 184-190 (2007).
- Burcu Akca, Ozge Guner, Mukaddes Can, Aysen Yilmaz and Deniz Uner, “Oxidation States and the Acidity of Ordered Arrays of Co–Pb Mixed Oxide Nanoparticles Templated in SBA15”, *Top Catal*, 49, 187–192 (2008).
- Chen, Y. S. and Cheng S., “Synthesis or Zr- incorporated SBA-15 Mesoporous Materials in a Self Generated Acidic Environment”, *Chem.Master*, 45, 4174 – 4180 (2004).



Chu W., Chernavskii P. A., Gengembre L., Pankina G. A., Fongarland P. and Khodakov A.Y., “Cobalt Species in Promoted Cobalt Alumina-supported Fischer-Tropsch Catalysts”, *J. Catal.*, 252, 215-230 (2007).

Ferenc Puskas, MD, PhD, Hilary P. Grocott, MD, FRCPC, William D. White, MPH, Joseph P. Mathew, MD, Mark F. Newman, MD, Shahar Bar-Yosef, MD, “Intraoperative Hyperglycemia and Cognitive Decline After CABG”, *Ann Thorac Surg*, 84, 1467-1473 (2007).

Girardon J. S., Constant-Griboval A., Gengembre L., Chernavskii P.A. and Khodakov A.Y., “Optimization of the Pretreatment Procedure in the Design of Cobalt Silica Supported Fischer-Tropsch Catalysts”, *Catal. Today*, 106, 161-165 (2005).

Hilmen A. M., Schanke D. and Holmen A., “TPR Study of the Mechanism of Rhenium Promotion of Alumina-supported Cobalt Fischer-Tropsch Catalysts”, *Catal. Lett*, 38, 143-147 (1996).

Iglesia E., “Design, Synthesis, and Use of Cobalt-Based Fischer-Tropsch Synthesis Catalysts”, *Applied Catalysis*, 161, 59-78 (1997).

Imre Puskas, Theo H. Fleisch, Jan B. Hall, Bernard L. Meyers and Robert T. Roginski, “Metal-support Interactions in Precipitated, Magnesium-promoted Cobalt\_silica Catalysts”, *Journal of Catalysis*, Volume 134, Issue 2, Pages 615-628 (April 1992).

- Jacobs G., Chaney J.A., Patterson P. M., Das T. K., Maillot J. C. and Davis B. H., “Fischer-Tropsch Synthesis: Study of the Promotion of Pt on the Reduction Property of Co/Al<sub>2</sub>O<sub>3</sub> Catalysts by in situ EXAFS of Co K and Pt LIII Edges and XPS”, *J. Synchrotron Radiat*, 11, 414-422 (2004).
- Jacobs G., Patterson P. M., Zhang Y., Das T., Li J. and Davis B. H., “Fischer-Tropsch Synthesis: Deactivation of Noble Metal Promoted Co/Al<sub>2</sub>O<sub>3</sub> Catalysts”, *Appl. Catal. A: Gen*, 233, 215-226 (2002).
- Junling Zhang, Jiangan Chen, Yongwang Li and Yuhan Sun, “Recent Technological Developments in Cobalt Catalysts for Fischer-Tropsch Synthesis”, *Journal of Natural Gas Chemistry*, 11, 99-108 (2002).
- Kababji A. H., B. Joseph, and J. T. Wolan, “Silica –Supported Cobalt Catalysts for Fisher-Tropsch Syhnthesis”, *Catal Letter*, 130, 72-78 (2009).
- Khodakov A. Y., Chu W., and Fongarland P, “Advances in the Development of Novel Cobalt Fischer-Tropsch Catalysts for Synthesis of Long-chain Hydrocarbons and Clean Fuels”, *Chem. Rev*, 107, 1692-1744 (2007).
- Khodakov A. Y, Lynch J., Bazin D., Rebours B., Zanier N., Moisson B. and Chaumette P., “Reducibility of Cobalt Species in Silica-supported Fischer-Tropsch Catalysts”, *J. Catal*, 168, 16-25 (1997).
- Li, B., Inagaki, S., Miyazaki, C. and Takahashi., H., “Synthesis of Highly Ordered Large Size Mesoporous Silica and Effect of Stabilization as Enzyme Supports in Organic Solvent”, *Chem. Res. Chinese Univ*, 18, 200 – 205 (2002).

- Martínez A., López C., Márquez F. and Díaz I., “Fischer-Tropsch Synthesis of Hydrocarbons Over Mesoporous Co/SBA-15 Catalysts: The Influence of Metal Loading, Cobalt Precursor, and Promoter”, *J. Catal*, 220, 486-499 (2003).
- Mauldin C. H. and Varnado D. E., “Rhenium as a Promoter of Titania-supported Cobalt Fischer-Tropsch Catalysts”, *Stud. Surf. Sci. Catal*, 136, 417-422 (2001).
- Mirji S. A., S. B. Halligudi, Dhanasri P. Sawant, Nalini E. Jacob., K. R. Patil, A. B. Gaikwad and S. D. Pradhan, “Adsorption of Octadecyltrichlorosilane on Mesoporous SBA-15”, *Applied Surface Science*, 252, 4097-4103 (2006).
- M. P. de Jong, I. Bergenti, W. Osikowicz, R. Friedlein, V. A. Dediu, C. Taliani, and W. R. Salaneck, “Valence Electronic States Related to  $Mn^{2+}$  at  $La_{0.7}Sr_{0.3}MnO_3$  Surfaces Characterized by Resonant Photoemission”, *Phys. Rev. B.*, Volume 73 (2006).
- Mukaddes CAN, Burcu A., Aysen Yilmaz and Deniz Uner, “Synthesis and Characterization of Co-Pb/SBA-15 Mesoporous Catalysts”, *Turk J Phys*, 287, 293 (2005).
- Perego, C. and Villa, P., *Catalysis Today*, 34, 281-305 (1997).
- Schanke D., Vada S., Blekkan E.A., Hilmen A.M., Hoff A. and Holmen A., “Study of Pt-Promoted Cobalt CO Hydrogenation Catalysts”, *J. Catal*, 156, 85-95 (1995).
- Schultz H., “Short History and Present Trends of Fisher Tropsch Synthesis”, *Appl. Catal. A.*, 186, 3-12 (1999).

Shalchi, W., "Gas to Liquid (GTL) Technology", *Society of Petroleum Engineer, Baghdad* (2006).

Shannon M. D., Lok C. M. and Casci J. L., "Imaging Promoter Atoms in Fischer-Tropsch Cobalt Catalysts by Aberration-corrected Scanning Transmission Electron Microscopy", *J. Catal*, 249, 41-51 (2007).

Storsaeter S., Borg Ø., Blekkan E.A. and Holmen A., "Study of the Effect of Water on Fischer-Tropsch Synthesis Over Supported Cobalt Catalysts", *J. Catal*, 231, 405-419 (2005).

Taguchi, A. and Schüth. F., "Microporous and Mesoporous Materials", 77, 1-45 (2005)

Tavasoli, Ahmad, Sadaghiani, Kambiz; Nakhaeipour, Ali; Ahangari and Masaumeh, "Cobalt Loading Effect on the Structure and Activity for Fisher-Tropsch and Water Gas Shift Reactions of Co/Al<sub>2</sub>O<sub>3</sub> Catalyst", *Iran J Chem J Eng*, 26, 1 (2007).

Timothy Biswick, William Jones, Alexandra Pacula, Ewa Serwicka and Jerzy Podobinski, "The Role of Anhydrous Zinc Nitrate in the Thermal Decomposition of the Zinc Hydroxyl Nitrate", *Journal of Solid State Chemistry*, 180, 1171-1179 (2007).

Tsubaki N., Sun S. and Fujimoto K., "Different Functions of the Noble Metals Added to Cobalt Catalysts for Fischer-Tropsch Synthesis", *J. Catal*, 199, 236-246 (2001).

Tuel, A., "Microporous and Mesoporous Materials", 27, 151-169 (1999).

- Vannice. M A., Plainfield; Robert L. Garten, Summit, both of N.J., “Hydrocarbon Synthesis from CO and H<sub>2</sub> using Ru Supported on a Titanium Oxide”, *Exxon Research Eng Co*, 4, 042-614 (1977).
- Wang, Y., Wang, X., Su, Z., Guo, Q., Tang, Q., Zhang, Q. and Wan, H., *Catalysis Today*, 93–95, 155–161 (2004).
- Wei D., Goodwin Jr. J. G., Oukaci R. and Singleton A. H., “Attrition Resistance of Cobalt F-T Catalysts for Slurry Bubble Column Reactor Use”, *Appl. Catal. A: Gen*, 210, 137-150 (2001).
- Xia, Y. and Mokaya, R., J., *Mater. Chem.* 13, 3112–3121 (2003).
- Xi Liang , Junhua , Qichun Lin and Keqin Sun, “Synthesis and Characterisation of Mesoporous Mn/Al-SBA-15 and its Catalytic for NO Reduction with Ammonia”, *Catalysis Communicatios*, 8, 1901-1904 (2007).
- Xueguang Wang, Kyle S. K. Lin .Jerry C. C.Chan, and Seofin Cheng, “Direct Synthesis and Catalytic Applications of Ordered Large Pore Aminopropyl-Functionalized SBA-15 Mesoporous Materials”, *J Phys ChemB*, 109, 1763-1769 (2005).
- Zhao, D., Huo, Q., Feng, J., Chmelka, B. F. and Stucky, G. D., “Nonionic Triblock and Star Diblock Copolymer and Oligomeric Surfactant Syntheses of Highly Ordered, Hydrothermally Stable, Mesoporous Silica Structures”, *Journal of the American Chemical Society*, 120, 6024-6036 (1998).

Zsoldos Z., Hoffer T. and Guzzi L., "Structure and Catalytic Activity of Alumina-supported Pt-Co Bimetallic Catalysts. 1. Characterization by X-ray Photoelectron Spectroscopy", *J. Phys. Chem*, 95, 798-801 (1991).

## APPENDICES A1

### Details Calculations

#### A1 Calculation of wt % zinc and cobalt loading using during incipient wetness impregnation method .

Additional information:

Molecular Weight Zinc Nitrate ( $\text{Zn}(\text{NO}_3)_2 \cdot 6\text{H}_2\text{O}$ ): 297.47 g/mol

Molecular Weight Zinc (Zn): 65.3g/mol

Molecular Weight Cobalt Nitrate ( $\text{Co}(\text{NO}_3)_2 \cdot 6\text{H}_2\text{O}$ ): 291.04 g/mol

Molecular Weight Cobalt (Co): 58.9 g/mol

Mass of SBA-15: 1gram

Equation used:

$$x \times \text{Molecular Weight} \frac{\text{Cobalt @Zinc (g)}}{\text{Cobalt nitrate @Zinc nitrate (g)}} = y(g) \rightarrow (1)$$

$$\frac{y(g)}{x + \text{Mass SBA-15}} = \text{wt \% needed} \rightarrow (2)$$

$y$  = Mass of Cobalt @ Zinc needed

$x$  = Mass of Cobalt Nitrate @ Zinc Nitrate needed

By using simultaneous equation, calculate  $x$  and  $y$ .

### A.1.1 Mass of Cobalt loaded to SBA-15.

Ratio of Co:Zn = 5 wt% :20 wt %

Calculation for 5-wt % Cobalt loaded is given below:

$$0.2024 x = y \rightarrow (1)$$

$$\frac{y}{x+1g} = 5 \text{ wt}\% \rightarrow (2)$$

by using simultaneous equation

$$x=0.328g$$

Ratio of Co:Zn = 10 wt% :20 wt %

Calculation for 10 wt % Cobalt loaded are given below:

$$0.2024 x = y \rightarrow (1)$$

$$\frac{y}{x+1g} = 10 \text{ wt}\% \rightarrow (2)$$

by using simultaneous equation

$$x=0.9766g$$

Ratio of Co:Zn = 15 wt% :20 wt %

Calculation for 15 wt % Cobalt loaded are given below:

$$0.2024 x = y \rightarrow (1)$$

$$\frac{y}{x+1g} = 15 \text{ wt}\% \rightarrow (2)$$

by using simultaneous equation

$$x=2.863g$$



**A.1.2 Mass of Zinc loaded to SBA-15**

Ratio of Co:Zn = 5 wt% :20 wt %

Ratio of Co:Zn = 10 wt% :20 wt %

Ratio of Co:Zn = 15 wt% :20 wt %

Calculation for 20 wt % zinc loaded to SBA-15 is given below:

$$0.21952 x = y \rightarrow (1)$$

$$\frac{y}{x+1g} = 20 \text{ wt}\% \rightarrow (2)$$

by using simultaneous equation

$$x=10.25g$$